Published by Institute of Physics Publishing for SISSA/ISAS
Received: *May 12, 2010*
Accepted: *May 12, 2010*

JHEP00(2010)000

A Scaling Relation of the Evolving Tidal Fields in a ΛCDM Cosmology

Jounghun Lee

Astronomy Program, FPRD, Department of Physics and Astronomy, Seoul National University, Seoul 151-747, Korea
E-mail: jounghun@astro.snu.ac.kr

Volker Springel

Max-Planck Institut fuer Astrophysik, Karl-Schwarzschild Strasse 1, D-85748 Garching, Germany
E-mail: volker@mpa-garching.mpg.de

Abstract: We report the finding of a scaling relation among the cosmic-web anisotropy parameter A, the linear density rms fluctuation $\sigma(r)$ and the linear growth factor $D(z)$. Using the tidal field derived from the Millennium Simulation on 512^3 grids at $z = 0,\ 2,\ 5$ and 127, we calculate the largest eigenvalues λ of the local tidal tensor at each grid resolution and measure its distance-averaged two-point correlation function, ξ_λ, as a function of the cosines of polar angles $\cos\theta$ in the local principal axis frame. We show that ξ_λ is quite anisotropic, increasing toward the directions of minimal matter compression, and that the anisotropy of ξ_λ increases as the redshift z decreases and as the upper distance cutoff r_c decreases. Fitting the numerical results to an analytic fitting model $\xi_\lambda(\cos\theta) \propto (1 + A\cos^n\theta)^{-1}$, it is found that the best fit value of A, dubbed the *cosmic-web anisotropy parameter*, varies systematically with $\sigma(r_c)$ and $D(z)$, allowing us to determine the simple empiral scaling relation $A(r_c, z) = 0.8\, D^{0.76}(z)\, \sigma(r_c)$.

Keywords: cosmic web, semi-analytic modeling.

Contents

1. Introduction

As confirmed by recent N-body simulations[1, 2], the large-scale spatial distribution of cold dark matter exhibits an anisotropic web-like pattern, which is often dubbed the *cosmic web*. The cosmic web of the dark matter distribution found in N-body simulations is also consistent with the observed large-scale filamentary distribution of galaxies in the real universe [3, 4]. According to the standard model of cosmic structure formation [5], the cosmic web originates in primordial density perturbations that are sharpened by gravitational tidal fields. The web becomes more anisotropic as the tidal fields become stronger due to the nonlinear processes during the gravitational evolution.

Various statistical tools have so far been proposed to describe the geometric properties of the cosmic web. For example, the conventional N-point statistics has been used to calculate the anisotropic spatial distribution of dark halos [6]. The Minkowski functionals have been employed to determine the morphological properties of the large-scale structures embedded in the cosmic web [7]. The N-dimensional skeleton approach has been found to be efficient in tracing the evolution of the cosmic web [8, 9]. The Multiscale Morphology Filter method has been applied to the large-scale galaxy distribution to identify the anisotropic structures of the cosmic web [10]. A method utilizing the concept of the *Local Dimension* has been suggested for the local quantification of the shapes of the galaxy neighborhood in the cosmic web [11]. The ellipticity-ellipticity correlations of dark halos have been used to quantify the large-scale anisotropy of the cosmic web [12]. Finally, tessellation techniques have been suggested to trace the evolution of the geometric structures in the universe [13, 14].

Very recently, it has been pointed out by Lee, Hahn and Porciani [15](LHP09, hereafter) that, since the cosmic web is produced by the anisotropic compression of matter

along the principal axes of the large-scale tidal fields, its anisotropic nature may be best quantified in the system of the principal axes of the tidal fields. This led them to suggest the anisotropic two-point correlations of the nonlinear traceless tidal field expressed in the principal axis frame, $\xi_\lambda(\mathbf{r})$, as a new statistical tool for the description of the cosmic web phenomenon.

Analyzing numerical data from high-resolution N-body simulations, they have determined $\xi_\lambda(\mathbf{r})$ and found that it has a much larger correlation length ($\sim 20\,h^{-1}$Mpc) and a higher degree of anisotropy than the density field itself. Integrating $\xi_\lambda(\mathbf{r})$ over distance r from 0 to a certain cut-off scale r_c, and expressing it as a function of the angle between the major principal axes and the separation vectors, they noted that the nonlinear traceless tidal field has a much higher degree of anisotropy than the nonlinear density field. Interestingly, the results of LHC09 imply that the correlations of the nonlinear traceless tidal field may have a link to the initial conditions.

Yet, the analysis of LHP09 was restricted to the present epoch and their results were obtained by setting the distance cutoff scale r_c to the correlation length of the nonlinear tidal field, $r_c = 20\,h^{-1}$Mpc. In this paper, our goal is to explore how the two-point correlations of the nonlinear traceless tidal field expressed in the principal axis system vary with redshift and distance scale by analyzing numerical data from high-resolution cosmological simulations. Throughout this paper, we assume a flat ΛCDM cosmology.

2. Physical Analysis

2.1 Construction of the Tidal Fields

For the construction of the tidal shear fields $T_{ij}(\mathbf{x})$, we use the density contrast fields $\delta(\mathbf{x})$ constructed on 512^3 pixels from the Millennium Simulation [1] by means of the count-in-cell method, at four different redshifts $z = 0,\ 2,\ 5$ and 127. The Millennium run [1] followed the evolution of the trajectories of 10^{10} dark matter particles, each of which has mass $8.6 \times 10^8\,h^{-1}M_\odot$, in a periodic box of linear size $500\,h^{-1}$Mpc, using a ΛCDM cosmology with the cosmological parameters $\Omega_m = 0.25,\ \Omega_\Lambda = 0.75,\ h = 0.73,\ \sigma_8 = 0.9$ and $n_s = 1$.

The Fourier-transform of the density field, $\delta(\mathbf{k})$, is obtained through the Fast-Fourier-Transformation (FFT) method [16]. Then, the Fourier transform of the tidal shear field, $T_{ij}(\mathbf{k})$, is calculated as $T_{ij}(\mathbf{k}) = k_i k_j \delta(\mathbf{k})/k^2$. The inverse Fourier-transformation of $T_{ij}(\mathbf{k})$ yields the tidal shear field in real space, $T_{ij}(\mathbf{x})$. The traceless tidal field is defined as $\tilde{T}_{ij}(\mathbf{x}) \equiv T_{ij}(\mathbf{x}) - \delta(\mathbf{x})/3$. At each pixel point we diagonalize $\tilde{T}_{ij}(\mathbf{x})$ to find its three eigenvalues and the corresponding eigenvectors. The local principal axis frame has the three eigenvectors as basis vectors with polar axis in the direction of the eigenvector corresponding to the smallest eigenvalue. The eigenvector corresponding to the largest (smallest) eigenvalue is parallel to the direction of maximal (minimal) compression of local matter distribution.

2.2 Correlations of the Traceless Tidal Fields

The two-point correlation function of the largest eigenvalue λ of the local tidal tensor at

redshift z is defined as [15]

$$\xi_\lambda(\mathbf{r}; z) = \langle \lambda(\mathbf{x}; z) \cdot \lambda(\mathbf{r} + \mathbf{x}; z) \rangle. \tag{2.1}$$

Let us express the separation vector $\mathbf{r}$ in terms of the spherical polar coordinates in the system of the principal axes of the local tidal tensor, $\mathbf{r} = (r,\ \cos\theta,\ \phi)$, with the polar axis aligned with the direction of minimum matter compression, i.e., the direction of the eigenvector corresponding to the smallest eigenvalue of $\tilde{T}_{ij}(\mathbf{x})$. If the λ-field was isotropic, then the two-point correlation $\xi_\lambda(\mathbf{r})$ would depend only on the separation distance r, but not on the polar and azimuthal angles θ and ϕ. The degree of the anisotropy of the cosmic web can be quantified by measuring how strongly ξ_λ changes with θ and ϕ. As the

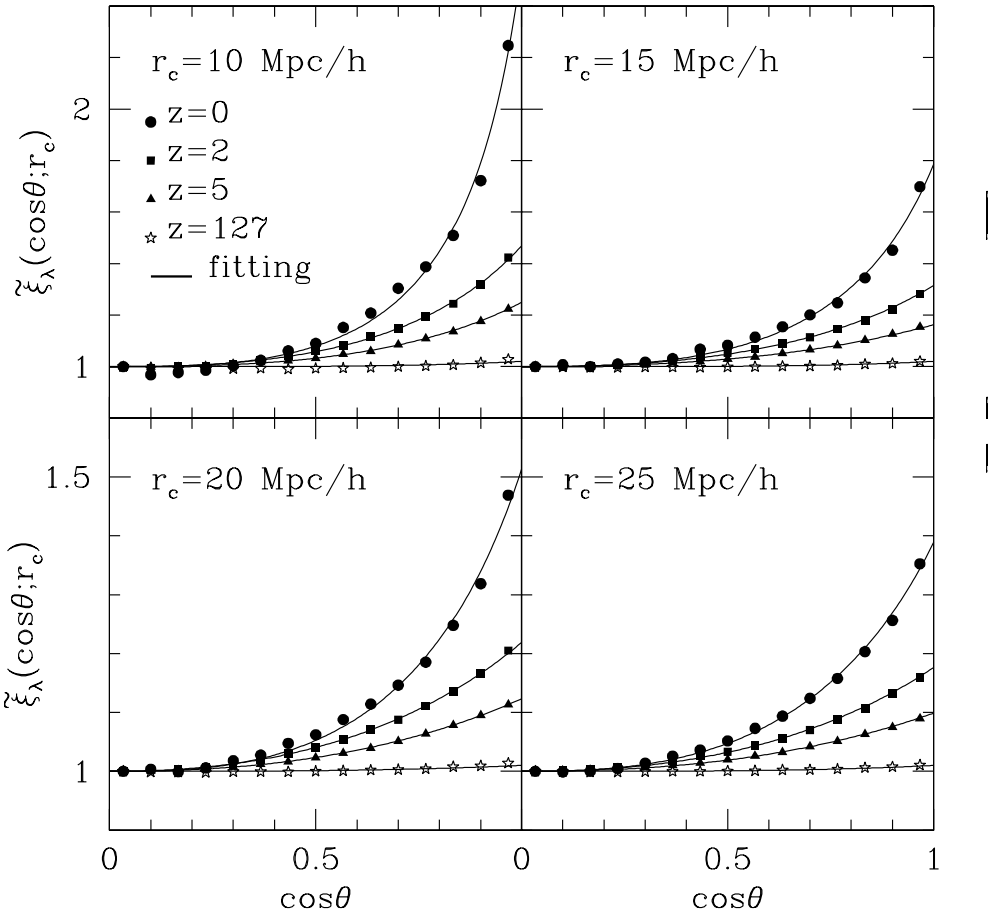

Figure 1: Anisotropic two point correlations of the lowest eigenvalues of the traceless tidal field in the tidal principal axis frame averaged over the distance up to r_c as a function of the cosine of the angles between the directions to the neighbor points and the eigenvectors corresponding to the lowest eigenvalues at four different redshifts ($z = 0,\ 2,\ 5$ and 127 as dots, square dots, triangles and asterisks, respectively), for the four different values of the distance cut-off scale $r_c = 10,\ 15,\ 20$ and $25\,h^{-1}$Mpc. In each panel, the thin solid lines represent the fitting models.

dependence of $\xi_\lambda(\mathbf{r})$ on the azimuthal angle ϕ has been found to be rather weak [15], here we focus mainly on the polar-angle dependence of $\xi_\lambda(\mathbf{r};z)$.

The anisotropic two-point correlation function of λ as a function of the cosines of the polar angles can be obtained by averaging $\xi_\lambda(\mathbf{r})$ over r and ϕ as

$$\xi_\lambda(\cos\theta) \equiv \int_0^{r_c} \mathrm{d}r \int_0^{2\pi} \mathrm{d}\phi\ \xi_\lambda(r,\cos\theta,\phi), \tag{2.2}$$

where r_c denotes the upper distance cutoff. When we integrate $\xi_\lambda(\mathbf{r})$ over r, we consider the distance cutoff scale r_c greater than $10\,h^{-1}$Mpc since $\xi_\lambda(\cos\theta)$ shows fluctuating unstable behavior at r_c less than $10\,h^{-1}$Mpc. It is expected that the degree of the anisotropy of $\xi_\lambda(\cos\theta)$ depends on the distance cutoff r_c and the redshift z, i.e., $\xi_\lambda(\cos\theta) = \xi_\lambda(\cos\theta; r_c, z)$.

Using the data from the Millennium simulation, we numerically measure $\xi_\lambda(\cos\theta; r_c, z)$ for the cases of four different distance cutoff scales, $r_c = 10,\ 15,\ 20$ and $25h^{-1}$Mpc, and at four different redshifts $z = 0,\ 2,\ 5$ and 127. For each pair of pixel points separated by $\mathbf{r}$, we first compute the product of the largest eigenvalues of the local traceless tidal tensors $\tilde{\mathbf{T}}$ and determine the polar and azimuthal angles of $\mathbf{r}$ in the local principal axes of the tidal tensor. Then, we take the spatial average of it to calculate the correlation of the largest eigenvalue $\xi_\lambda(\mathbf{r};z)$. Finally, we determine the expression of the correlation as a function of the cosine of the polar angle by averaging $\xi_\lambda(\mathbf{r};z)$ over the azimuthal angle ϕ and over distance r from 0 to r_c. For the detailed explanation on how to measure $\xi_\lambda(\cos\theta)$ from numerical data, we refer the readers to LHP09 [15].

Figure 1 plots the rescaled anisotropic two-point correlation of the traceless tidal fields, $\tilde{\xi}_\lambda(\cos\theta) \equiv \xi_\lambda(\cos\theta)/\xi_\lambda(0)$, for $r_c = 10,\ 15,\ 20$ and $25\,h^{-1}$Mpc (in the top-left, top-right, bottom-left and bottom-right panels, respectively) at $z = 0,\ 2,\ 5$ and 127 (dots, squares, triangles and open stars, respectively). In each panel, the solid lines correspond to the fitting models described in section 3.1. As it can be seen, $\tilde{\xi}_\lambda(\cos\theta; r_c, z)$ increases with $\cos\theta$ at all redshifts for all cases of r_c, indicating that the λ-field is anisotropic and more strongly correlated along the directions of minimum compression of dark matter in the local frame, which is consistent with the trend found by LHP09.

The standard deviations on the numerical measurement of $\tilde{\xi}_\lambda(\cos\theta)$ are also calculated as statistical noises, which turn out to be as small as $\leq 10^{-5}$ for all cases. Although it would be desirable to estimate jackknife error bars that include not only the statistical noise but also the cosmic variance, it is difficult to estimate them here since dividing the simulation box would destroy the periodicity of the box needed for our Fourier-based calculation of the tidal field. Hence, we omit the errorbars in Fig. 1 since the calculated statistical errors are anyway invisibly small.

3. Results

3.1 Fitting Formula

Noting that $\tilde{\xi}_\lambda(\cos\theta; r_c)$ increases with $\cos\theta$, we employ the following fitting model for it [15]:

$$\tilde{\xi}_\lambda(\cos\theta, z; r_c) = \frac{1}{1 + A\cos^n\theta}, \tag{3.1}$$

where A and n are two adjustable parameters. Fitting Equation (3.1) to the numerical results with the help of the χ^2-minimization method, we determine the best-fit values of A and n for each case of r_c at each redshift. For the calculation of χ^2, we set the values of all errors associated with the numerical measurements to unity rather than to the corresponding standard deviations of $\tilde{\xi}_\lambda$ [17], since the standard deviations are found to be extremely small in our case and do not account for cosmic variance, as discussed in section 2.2. Table 1 lists the best-fit values obtained for A and n at $z = 0$ for the four different values of r_c, while in Table 2 we provide the best-fit values of A and n at four different redshifts, setting r_c to $20\,h^{-1}$Mpc.

r_c [h^{-1}Mpc]	A	n
10	0.61	3.05
15	0.43	2.8
20	0.34	2.77
25	0.28	2.63

Table 1: Best-fit values of A and n at $z = 0$ for the four distance cut-off scales r_c.

redshift	A	n
0	0.34	2.77
2	0.18	2.21
5	0.11	2.26
127	0.01	3.1

Table 2: Best-fit values of A and n with $r_c = 20\,h^{-1}$Mpc at four different redshifts.

Each panel of Fig. 1 shows the fitting models of $\tilde{\xi}_\lambda$ with the best-fit values of A and n as thin solid lines. It can be seen that Eq. (3.1) indeed provides excellent fits to the numerical results for all values of r_c at all redshifts. In all cases the minimum values of χ^2 are formally found to be smaller than 10^{-3}. The parameter A is dubbed the *cosmic-web anisotropy parameter*, as it measures the strength of the dependence of $\tilde{\xi}_\lambda$ on $\cos\theta$. If the λ-field was isotropic, A would be zero. The more anisotropic the cosmic web is, the higher the value of this parameter A. Regarding the other fitting parameter n, it also shows a monotonic decrease with r_c, but no systematic change with redshift z. Therefore, we focus mainly on the cosmic web anisotropy parameter A from here on.

It is worth comparing Eq. (3.1) with the fitting model given in LHP09, who defined the polar angle as the angle between $\mathbf{r}$ and the eigenvector corresponding to the *largest* eigenvalue. In this work, we define the polar angle as the angle between $\mathbf{r}$ and the eigenvector corresponding to the *smallest* eigenvalue. The reason for using a different definition of the polar axis here is that ξ_λ is found to exhibit more obvious anisotropic behavior when the polar axis is chosen to be parallel to the direction of the eigenvector corresponding to the smallest eigenvalue. In addition, we also vary the power of $\cos\theta$ in the fitting model, while in LHP09 this was kept fixed.

3.2 A Scaling Relation

Noting a systematic trend in the variation of the cosmic-web anisotropy parameter A with r_c and z, we investigate how A depends on the linear density rms fluctuation $\sigma(r_c)$ smoothed on the distance cut-off scale r_c, and on the linear growth factor $D(z)$. Using various distance cut-off values equal to $r_c = 10,\ 12,\ 14,\ 16,\ 20$ and $25\,h^{-1}$Mpc at each redshift, we measure numerically $\tilde{\xi}_\lambda(\cos\theta; r_c)$ by using the data from the Millennium Simulation and

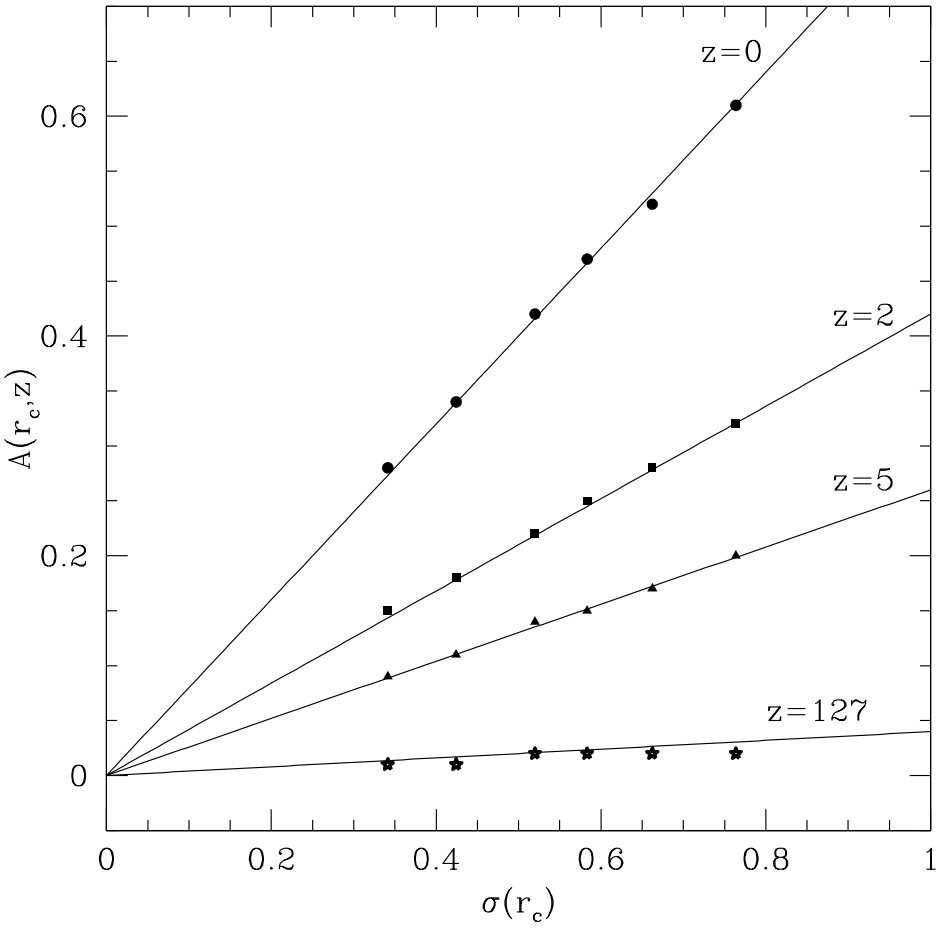

Figure 2: Scaling relations between the cosmic web anisotropy parameter A and the linear density rms density fluctuations on the distance cutoff scale r_c at $z = 0,\ 2,\ 5$ and 127.

by determining the best-fit value of A through χ^2 fitting of Eq. (3.1) to the numerical data points in each case.

We also analytically compute the linear density rms fluctuations $\sigma(r_c)$ smoothed on the same distance cut-off scale r_c as

$$\sigma^2(r_c) = \int_{-\infty}^{\infty} \Delta^2(k) W^2(kr_c) d\ln k, \tag{3.2}$$

where $W(kr_c)$ is the top-hat filter of scale radius r_c and $\Delta^2(k)$ is the dimensionless linear matter power spectrum. The following analytic approximation for $\Delta^2(k)$ given by [18] is used:

$$\Delta^2(k) \propto k^{n_s+3} \left[\frac{\ln(1+2.34q)}{2.34q}\right]^2 [1+3.89q+(16.1q)^2+(5.46)^3+(6.71q)^4]^{-1/2}, \tag{3.3}$$

where $q \equiv k/[\Omega_m h^2 \mathrm{Mpc}^{-1}]$ [19] and n_s is the spectral index of the primordial power spectrum. For the case that the key cosmological parameters (Ω_m, h and σ_8) are set at the

values used by the Millennium run, this formula turns out to agree sufficiently well with the result from the CMBFAST code [20].

Figure 2 plots the best-fit values of A for the six different values of r_c versus the linear rms density fluctuations $\sigma(r_c)$ smoothed on the same scale, at the four different redshifts we considered. This plot reveals that the cosmic-web anisotropy parameter A is directly proportional to $\sigma(r_c)$. The cosmic web anisotropy parameter A is shown to decrease monotonically with z, quantifying the evolution of the anisotropy of the traceless tidal fields. Note that this result is consistent with the qualitative explanation of the cosmic web theory [5].

It is interesting to see in Fig. 2 that $A[\sigma(r_c)]$ at each redshift is well described by a straight line, and that the slope of the line decreases with z. Supposing $A \propto \sigma(r_c)$, we investigate how the proportionality factor between A and $\sigma(r_c)$ (i.e., the slope of the straight line) changes with the linear growth factor $D(z)$. For the evaluation of the linear growth factor $D(z)$, we use the formula given in [21].

$$D(z) \propto \frac{5}{2}\Omega_m[\Omega_m(1+z)^3+\Omega_\Lambda]^{1/2}\int_z^\infty dz' \frac{1+z'}{[\Omega_m(1+z')^3+\Omega_\Lambda]^{3/2}}. \tag{3.4}$$

We numerically calculate the ratio, $A/\sigma(r_c)$, at each redshift. Fitting $A/\sigma(r_c)$ to a power-law formula $\alpha D^\beta(z)$ and determining the best-fit value of α and β at each redshift with the help of the χ^2 statistics, we find that the ratio $A/\sigma(r_c)$ varies as $0.8\,D^{0.76}(z)$. Fig. 3 plots $A(r_c,z)/\sigma(r_c)$ versus $D(z)$. The numerical results of $A(r_c,z)/\sigma(r_c)$ at four redshifts are shown as circles while the fitting model $0.8\,D^{0.76}(z)$ is shown as a solid line. This result demonstrates that the numerically obtained ratio between A and $\sigma(r_c)$ is indeed well fitted by $0.8D^{0.76}(z)$.

Finally, we can combine these findings into the following scaling relation among cosmic web anisotropy parameter $A(r_c,z)$, linear density rms fluctuation $\sigma(r_c)$ on the scale of r_c, and linear growth factor $D(z)$:

$$A(r_c,z) = 0.8\,D^{0.76}(z)\sigma(r_c). \tag{3.5}$$

This scaling relation quantifies how the cosmic web anisotropy parameter increases as the Universe evolves, revealing a link between the initial conditions and the anisotropic clustering of the nonlinear traceless tidal field expressed in the principal axis frame.

4. Discussion

To quantify the web-like pattern in the large-scale matter distribution, we have introduced the new concept of the cosmic web anisotropy parameter, which measures the degree of the anisotropy of the two-point correlations of the largest eigenvalues of the traceless tidal fields in the principal-axis frame. By analyzing the numerical data from the Millennium Simulation at different redshifts, we have empirically found a simple scaling relation among the cosmic web anisotropy parameter, the linear density rms fluctuations and the linear growth factor. Our results have allowed us to quantify how the anisotropy of the traceless

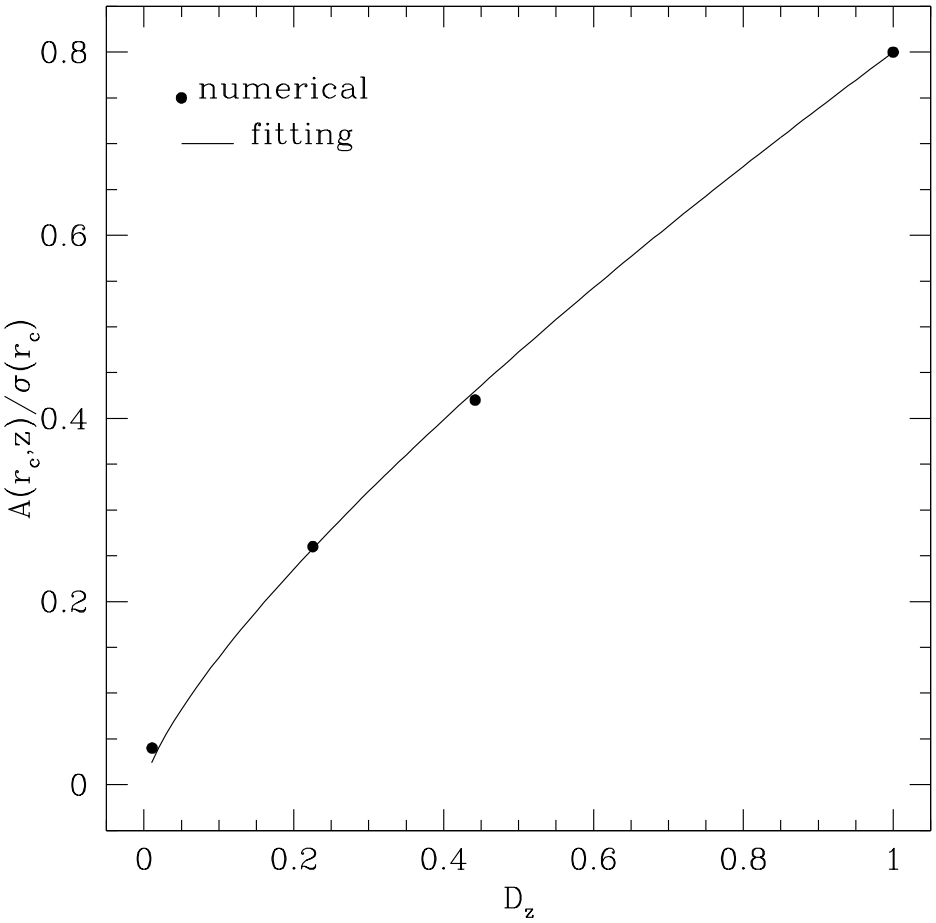

Figure 3: Scaling relation between $A(r_c, z)/\sigma(r_c)$ and the linear growth factor D_z.

tidal fields increases as the growth factor and the linear density rms fluctuations increase. This new scaling relation thus provides a measure for the growth of anisotropy in the evolving cosmic web of the Universe.

The simple functional forms we found for the correlation and the scaling relation (eqs. [3.1] and [3.5]) suggest that there might exist a simple explanation for these functional forms in linear perturbation theory. Yet, we have not been able to develop such a theory thus far, as the analytic treatment from first principles turns out to be extremely hard since we deal here with the *nonlinear* two-point correlations measured in the *principal* axis frame.

A crucial implication of our result is that the anisotropy of the cosmic web may be produced by three competing effects. The trace part of the tidal field and the cosmic expansion tend to make the matter distribution more isotropic, whereas the traceless part of the tidal field stretches the matter distribution and induces large-scale anisotropy. The competition among these three effects imprints the web-like pattern in the large-scale matter distribution, just as the competition between gravity and radiation pressure has left imprints in the

form of acoustic oscillations in the temperature map of the cosmic microwave background radiation [22].

Since the linear growth factor $D(z)$ and the linear density rms fluctuations $\sigma(r_c)$ are functions of the primary cosmological parameters such as the dark energy equation of state parameter w and the density parameter Ω_m, our results also hint that the cosmic web anisotropy parameter may be a new probe of cosmology. Given the scaling relation (eq.[3.5]), we expect that if the cosmic web anisotropy parameter A is measured for two different distance cut-off scales r_c at the same redshift, it may be possible to put a constraint on the density parameter Ω_m by taking the ratio between the two values, removing the parameter degeneracy with the amplitude of the linear power spectrum σ_8. Similarly, by measuring the cosmic web anisotropy parameter at two different redshifts and taking the ratio between the two values, a constraint on the dark energy equation of state parameter w results.

The success of using the cosmic web anisotropy parameter as a new cosmological probe, however, is contingent upon a couple of future tests. First of all, it needs to be examined whether or not the same scaling relation also holds for different cosmologies since we have derived it assuming a ΛCDM cosmology with a specific set of cosmological parameters. Secondly, what is readily measurable in practice is not the tidal field of the dark matter distribution but that of the galaxy distribution. It will hence be necessary to investigate how the bias between light and matter affects the scaling relation. We investigate this question in forthcoming work, and hope to report the results elsewhere in the near future.

Acknowledgments

The Millennium Simulation data used in this work are available at http://www.mpa-garching.mpg.de/millennium. We thank an anonymous referee for helpful suggestions. J.L. is very grateful to S.D.M.White and the Max-Planck-Institute for Astrophysicsat in Garching for the warm hospitality where this research was initiated. J.L. acknowledges financial support from the Korea Science and Engineering Foundation (KOSEF) grant funded by the Korean Government (MOST, NO. R01-2007-000-10246-0).

References

[1] Springel V et al., *Simulations of the formation, evolution and clustering of galaxies and quasars*, 2005 *Nature* **435** 629

[2] Faucher-Giguere C A, Lidz A and Hernquist L, *Numerical Simulations Unravel the Cosmic Web*, 2008 *Science* **319** 52

[3] Colless M et al., *The 2dF Galaxy Redshift Survey: spectra and redshifts*, 2001 *Mon.Not.Roy.Astron.Soc.* **328** 1039

[4] Strass M A, Weinberg D H, Lupton R H and the SDSS collaboration, *Spectroscopic Target Selection in the Sloan Digital Sky Survey: The Main Galaxy Sample*, 2002 *Astron. J.* **124** 1810

[5] Bond J R, Kofman L and Pogosyan D, *How filaments of galaxies are woven into the cosmic web*, 1996 *Nature* **380** 603

[6] Bond J R and Myers S T, *The Peak-Patch Picture of Cosmic Catalogs. I. Algorithms*, 1996 *Astrophys. J.* **103** 1

[7] Schmalzing J, Buchert T, Melott A L , Sahni V, Sathyaprakash B S and Shandarin S F, *Disentangling the Cosmic Web. I. Morphology of Isodensity Contours* , 1999 *Astrophys. J.* **526** 568

[8] Sousbie T, Pichon C, Colombi S, Novikov D and Pogosyan D, *The 3D skeleton: tracing the filamentary structure of the Universe*, 2008 *Mon.Not.Roy.Astron.Soc.* **383** 1655

[9] Sousbie T, Colombi S and Pichon C, *The fully connected N-dimensional skeleton: probing the evolution of the cosmic web*, 2009 *Mon.Not.Roy.Astron.Soc.* **393** 457

[10] Arago-Calvo M A, Jones B J T, van de Weygaert R and van der Hulst J M, *The multiscale morphology filter: identifying and extracting spatial patterns in the galaxy distribution*, 2007 *Astron. and Astrophys.* **474** 315

[11] Sarkar P and Bharadwaj S, *The Local Dimension: a method to quantify the Cosmic Web*, 2009 *Mon.Not.Roy.Astron.Soc.* **394** 66

[12] Lee J, Springel V., Pen U L and Lemson G, *Quantifying the cosmic web - I. The large-scale halo ellipticity-ellipticity and ellipticity-direction correlations*, 2009 *Mon.Not.Roy.Astron.Soc.* **386** 1266

[13] Shandarin S F, *Tessellating the Universe: the Zel'dovich and Adhesion tiling of space*, 2009 [arXiv:0912.4520]

[14] Shandarin S F, Habib S, Heitmann K, *Origin of the Cosmic Network: Nature vs Nurture*, 2009 [arXiv:0912.4471]

[15] Lee J, Hahn O and Porciani C, *The Anisotropic Two-Point Correlation Functions of the Nonlinear Traceless Tidal Field in the Principal-Axis Frame*, 2009 *Astrophys. J.* **705** 1469

[16] Press W H, Teukoksky S A, Vetterling W T and Flannery B P, *Numerical Recipes in FORTRAN*, 1992 Cambridge Univ. Press

[17] Bevington P R and Robinson D K, *Data Reduction and Error Analysis for the Physical Sciences*, 1996 McGraw-Hill Press

[18] Bardeen J M, Bond J R, Kaiser N, and Szalay A S, *The Statistics of the Peaks of Gaussian Random Fields*, 1986 *Astrophys. J.* **304** 15

[19] Peacock J A and Dodds S J, *Reconstructing the Linear Power Spectrum of Cosmological Mass Fluctuations*, 1994 *Mon.Not.Roy.Astron.Soc.* **267** 1020

[20] Seljak U and Zaldarriaga M, *A Line-of-Sight Integration Approach to Cosmic Microwave Background Anisotropies*, 1996 *Astrophys. J.* **469** 437

[21] Lahav O, Lilje P B, Primack J R and Rees M J, *Dynamical effects of the cosmological constant* 1991 *Mon.Not.Roy.Astron.Soc.* **251** 128

[22] Hu W and Sugiyama N, *Anisotropies in the cosmic microwave background: an analytic approach*, 1995 *Astrophys. J.* **444** 489